# AN EXPERIMENTAL INVESTIGATION OF WIND TUNNEL WALL INTERFERENCE ON ROLLING AND YAWING MOMENTS DUE TO DEFLECTED AILERONS.

T H E S I S

by

WALTER L. KOCH

In Partial Fulfillment of the Requirements for the Degree of

MASTER OF SCIENCE in AERONAUTICAL ENGINEERING

California Institute of Technology

Pasadena, California

1939

## ACKNOWLEDGEMENTS

The author wishes to express his gratitude to Drs. Theodore von Karman and C.B. Millikan for the suggestion of the subject of this research.

Grateful acknowledgement is also made to Drs. E.S. Seehler and A.L. Klein for their valuable advice during the design of the equipment and to Dr. W.R. Sears and Mr. H.J. Stewart for their helpful criticism during the course of the work.

TABLE OF CONTENTS

## SUMMARY

Wind tunnel tests were made on a model wing with deflected ailerons in both open- and closed-jet configurations of a small wind tunnel. Rolling and yawing moments and lift were measured at various angles of attack. The wind tunnel wall interference on rolling and yawing moments is determined by comparison of the open- and closed-jet results. An approximate comparison with available theories is included. It appears that the interference effects measured are somewhat smaller than predicted by the theories.

## INTRODUCTION

In testing airplane models in the wind tunnel it has been found that the results obtained differ somewhat from the data derived from flight tests of full size airplanes in free air. This is partly due to the phenomenon of wind tunnel wall interferences.

In order to reduce the wind tunnel results to free air conditions and thus give the airplane designer a means of predetermining the characteristics of the full size airplane, certain corrections must be made on the moments and forces measured on the model.

Theories have been developed for correcting wind tunnel results for tunnels of various cross-sectional shapes. One of the most recent investigations of this kind is reported in a paper by H.J. Stewart (Reference 1), which gives the theoretical values of the wind tunnel wall interference on yawing moments due to aileron deflections. Since the values obtained by Stewart are fairly large in many practical cases, the present research was undertaken with the primary object of obtaining an experimental check on Stewart's results. In the

course of the tests it was possible to investigate simultaneously the wall effect on rolling moments, thus affording an experimental check of the corresponding theory of M.A. Biot (Reference 2).

The method used in these tests is based on the theoretical result (cf. References 1 and 2) that the interference effects for open- and closed-jet tunnels of the same cross-sections are equal in magnitude and opposite in sense. The results of identical tests in the open- and closed-jet configuration of a wind tunnel are compared; the difference between them is equal to twice the interference effect.

Since the tunnel available for these tests had a square cross-section, the comparison with Stewart's and Biot's theories which are calculated for circular tunnels can be only approximate. However, analogous theoretical calculations, based on the same assumptions, but for a square tunnel, are in progress at California Institute of Technology, and a more exact comparison will be possible shortly.

## DESCRIPTION OF EQUIPMENT AND TESTS

THE MODEL:

The wing used was of symmetrical profile NACA 0018. The ailerons were of the unbalanced type, the hinge being a thin sheet of copper extending halfway into wing and aileron. (See Fig. 1).

This copper strip was sufficiently rigid to keep the aileron setting constant even at high tunnel speeds.

DIMENSIONS:

| | |
|---|---|
| Material: | Mahogany |
| Wing Area: | 36 sq. in. |
| Span: | 12 in. |
| Aspect Ratio: | 4 |
| Taper Ratio: | 1:2 |
| Center Chord: | 4 in. |
| Tip Chord: | 2 in. |
| Thickness at Center: | 0.71 in. |
| at Tips: | 0.16 in. |
| AILERONS, length: | 3 in. |
| $a_1$ | 2½ in. |
| $a_2$ | 5½ in. |
| Chord: | About 30% of wing chord. |

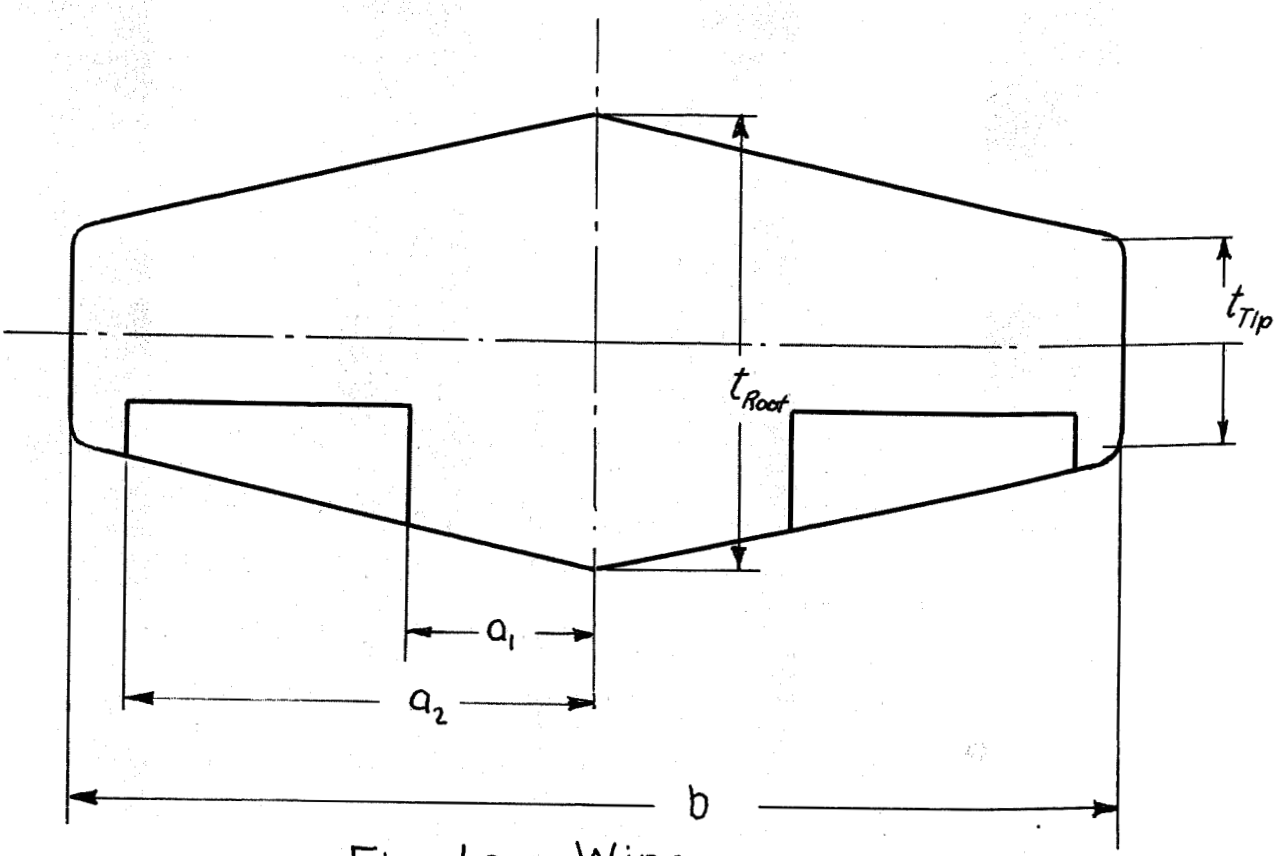


Fig. 1a. Wing.

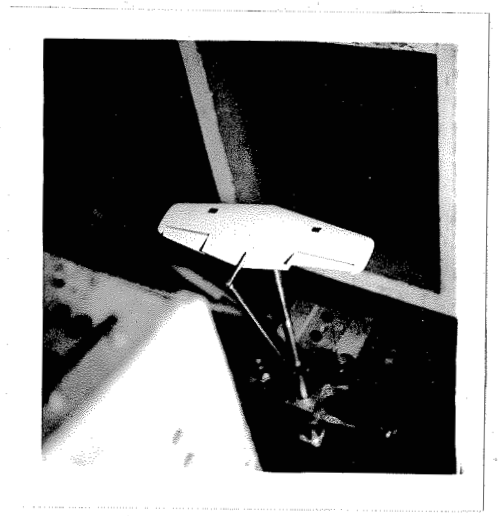

Fig. 1 Model Wing.

## THE WIND TUNNEL

The experiments were carried out in a tunnel of the return type (Reference 3, Fig. 2) powered by a 15 HP. AC motor, giving the air a maximum speed of about 140 m.p.h.

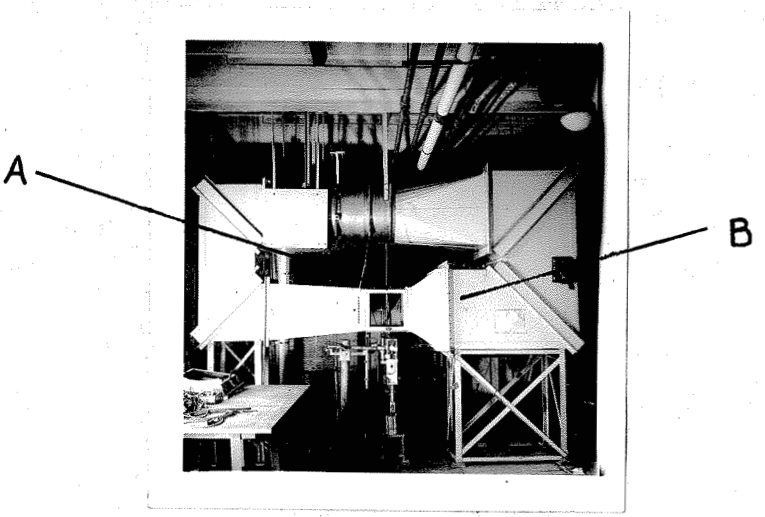


Fig. 2: The Wind Tunnel.

The square working section had a width and height of 14 in. leaving a clearance of 1 in. between the wing tips of the model and the walls. In order to allow inspection of the model during tests with closed jet, the side walls of the working section were formed by two large glass windows (Fig. 3).

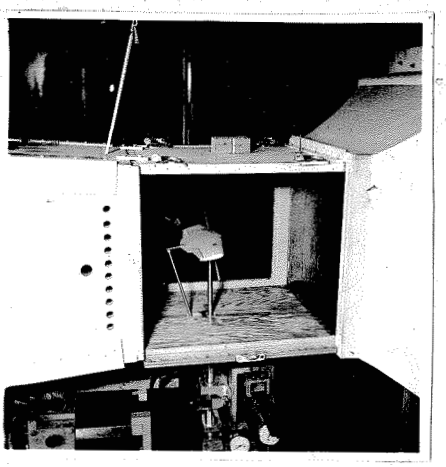

Fig. 3: Wind Tunnel at Closed Jet.

These windows and the upper and lower wall of the working section were designed such that for runs with open jet the whole section could be taken off the tunnel without the need of detaching the suspension system of the model, thus leaving model as well as balances and dial gauges completely unchanged for comparison tests with open and closed jet.

For open jet runs the intake nozzle of the jet was equipped with a collector ring with its walls set at an angle of 45° to the airstream (Fig. 4).

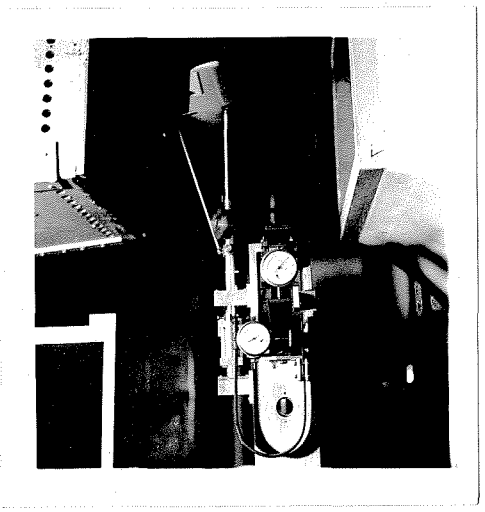

Fig. 4: Wind Tunnel at Open Jet.

After the first test runs, however, it was observed that a large vortex was created by the collector ring, which tended to distort the straight flow of the streamlines.

To eliminate this undesirable phenomenon boards of $1\frac{1}{8}$ in. width were attached to the outer edges of the ring at a right angle to the boards of the ring (Fig. 5) whereafter the large eddies almost entirely vanished.

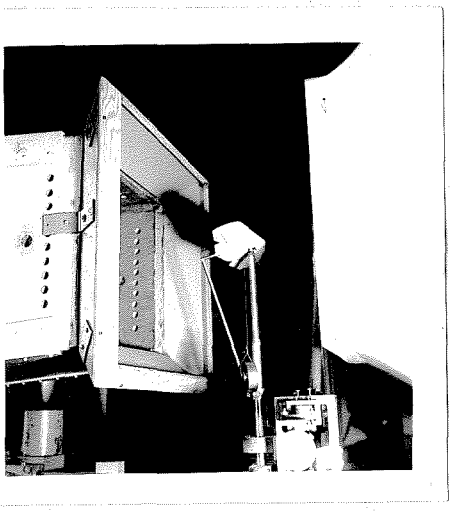

Fig. 5: Collector Ring.

As a measure of the wind tunnel speed the difference in static pressure between the two points A and B (See Fig. 2) was used in the case of the closed jet, and that between the point B and the surrounding room was used in the case of the open jet. These were calibrated against the dynamic pressure in the jet as described later. The static pressure difference is denoted by $h_s$.

## THE BALANCE SYSTEM

Since the measurement of the drag in these tests was unimportant, the balances measured only three components: lift, yawing moment, and rolling moment. At about 30% from the leading edge on the ℄ the wing was supported by a single shaft in such a way as to allow free rotation in pitch as well as yaw.

The vertical shaft carrying the model at its top was mounted on two ball bearings about 6 in. apart, allowing the wing to rotate freely in yaw. A lever arm attached to the shaft deflected the end of a U-spring with which a dial gauge was connected. The readings of the gauge, calibrated in in. lbs., gave a direct measure of the yawing moment (Fig. 6).

A second lever extending from the shaft formed the support for another U-spring, whose dial gauge measured the rolling moment of the wing. Two thin wires attached to the wing on the pitching axis at a distance of 3 in. from the ℄ on both sides transferred the rolling moment of the wing to the balance. One wire was fastened to the U-spring, the other carried a small steel weight to give the U-spring a pretension. The rolling moment component was attached rigidly to the vertical shaft, thus following freely the yawing rotation and measuring rolling moments independent of the yawing motion.

Both roll and yaw components were mounted on a block which was free to swing up and down. The block was suspended from a spring to which a dial gauge was attached. This gauge read the lift force. To assure straight up-and-down motion for the wing, the lift block was guided by struts extending about four feet from a pole. The pole was anchored in the ground, thus carrying the whole balance system and eliminating disturbing vibrations. (Fig. 6).

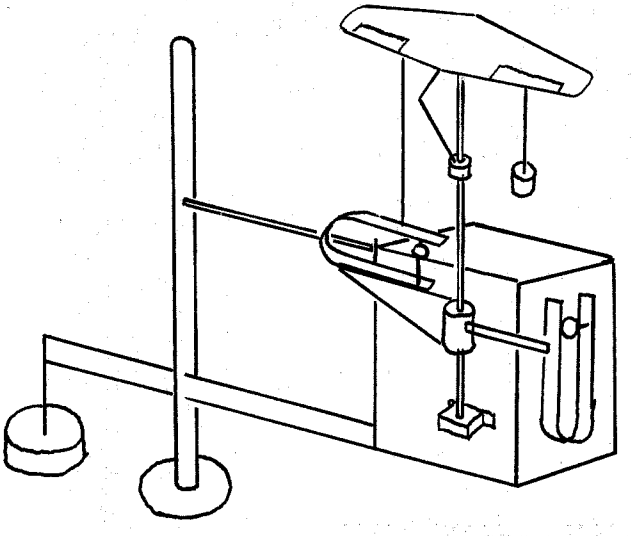

Fig. 6: Balance System (Schematically).

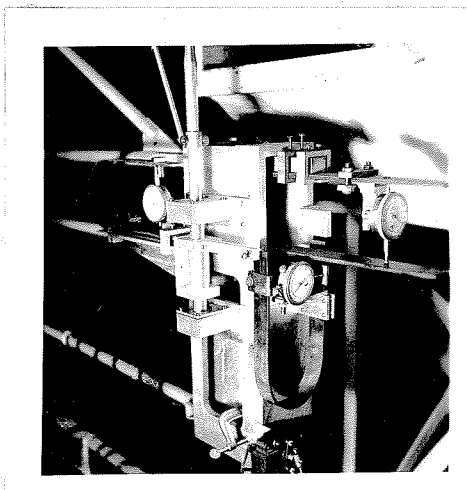

Fig. 7.

## CALIBRATION OF TUNNEL AND BALANCES

A. TUNNEL.

CLOSED JET.

In order to find the velocity distribution over the width of the tunnel and determine the "averaging factor", a velocity survey was made using a standard Prandtl pitot tube. Since the velocity pattern could be assumed symmetrical about the $\mathcal{L}$ of the tunnel, only the half width of the working section was investigated.

As Fig. 8 shows, the air speed was kept at a q of about 8 cm. The velocity pattern shows a slight variation, having its maximum value in the center ($q_c$ = 7.99 cm.) and its minimum at approximately two thirds of the half width from the center. The mean q over the wing span was found to be $q_{mean}$ = 7.92, thus giving an averaging factor:

$$A.F. = \frac{q_{mean}}{q_c} = \frac{7.92}{7.99} = 0.99$$

In order to convert the manometer readings $h_s$ into the actual q at which the tunnel was running, a $q/h_s$ calibration was made which is shown in Fig. 9. (Since it was found that the density of the manometer fluid did not vary, all values of $h_s$ are in terms of fluid of a constant density).

Over the range of $h_s$, at which most runs were made, a 3 cm. $< h_s <$ 4 cm., the factor $q/h_s$ is approximately constant, $q/h_s = .94$ .

OPEN JET.

The velocity distribution over the width of the tunnel at open jet was so uniform, Fig. 10, that it was unnecessary to apply an averaging factor.

Fig. 11 shows the factor $q/h_s$ plotted against $h_s$ for open jet. Over the range of $h_s$, at which the tests were made $3 < h_s < 4$, it can be assumed to be constant, $q/h_s = .88$ .

B. BALANCES.

Dial gauges attached to the U-springs, registering deflections as small as $\frac{1}{100}$ mm., appeared to be the best means of measuring the forces for these investigations (Fig. 7).

They were calibrated by weights attached to the U-springs by a string hanging over a pulley. The figures 11, 12 and 13 show the calibration curves for lift-gauge, yawing and rolling moment gauges.

The location of the wing in the working section in open jet tests differed somewhat from that at closed jet runs such that in the former case the moment arm of the yawing component was increased slightly. This explains the higher calibration curve for open jet yaw readings.

## EXPERIMENTAL PROCEDURE

The wing was tested with both ailerons deflected to equal and opposite settings. The first series of runs was made with an aileron angle a = 14° in both open and closed working sections.

During all tests the yaw angle of the model was zero whereas the angle of attack was varied.

In the second series of runs the aileron angle was changed to a = 21° and kept constant throughout the tests in both open and closed jets. Here again the model was varied in pitch, the yaw angle being kept zero. During preliminary runs it was found that the optimum speed of the tunnel at which the model did not flutter, was 3 cm. $< q <$ 4 cm., corresponding to an air velocity V of approximately 60 m.p.h. Hence all tests in this investigation were made within this speed range.

## SAMPLE CALCULATION

Closed Jet Run (Curve Fig. 12, Point 2)

Aileron Angle $a = 14^0$

Span $b = 12$ in.

Wing Area $S = 36$ in.$^2$

Gauge Readings:

Lift = 12

Yaw = 99.4

Roll = 74

Manometer Reading $h_s$ = 2.55 cm. (fluid density same as in calibration tests)

$q/h_s$ = .94 gr/cm.$^3$

Averaging Factor A.F. = .99

a) Calculation of $q_{av}$:

$q_{av}$ = A.F. x $q_o$ gr/cm.$^2$

$q_o = h_s \times q/h_s$ gr/cm.$^2$

$= .0142\ h_s \times q/h_s$ #/in.$^2$

$q_{av} = .99 \times .0142 \times 2.55 \times .94$ #/in.$^2$

$q_{av} = .0336$ #/in.$^2$

b) Lift Coefficient $C_L$:

Gauge Reading: 12 gives L = .28 lbs. (Calibration Curve Fig. 21)

$$C_L = \frac{L}{S \times q/av} = \frac{.28}{36 \times .0336} = .23$$

c) Yawing Moment Coefficient $C_y$.

Gauge Reading: 99.4 gives $M_y$ = -.02 in. lbs. (Calibration Curve Fig. 22)

$$C_y = \frac{M_y}{S \times q \times b} = -\frac{.02}{36 \times .0336 \times 12} = \underline{\underline{-.0014}}$$

d) Rolling Moment Coefficient $C_R$.

Gauge Reading: 74 gives $M_R$ = .77 in. lbs. (Calibration Curve Fig. 23)

$$C_R = \frac{M_R}{S \times q \times b} = \frac{.77}{36 \times .0336 \times 12} = \underline{\underline{.053}}$$

The following tables give the numerical values for the two sample curves shown in Fig. 12, 13. Enough data is tabulated to allow checking of every step.

Tabulated Values:

1) Run 2, closed jet (Fig. 12).

| Lift Gauge | L (lbs.) | Yaw Gauge | $M_y$ (in.lbs.) | Roll Gauge | $M_R$ (in.lbs.) | h | q | $C_L$ | $C_y$ | $C_R$ |
|---|---|---|---|---|---|---|---|---|---|---|
| 12 | .28 | 99.4 | .020 | 74.0 | .77 | 2.55 | .0336 | .23 | .0014 | .053 |
| 18 | .43 | 98.7 | .041 | 74.0 | .77 | 2.55 | .0336 | .36 | .0028 | .053 |
| 29 | .68 | 97.8 | .066 | 72.5 | .80 | 2.55 | .0336 | .56 | .0046 | .055 |
| 39 | .92 | 97.0 | .085 | 73.5 | .78 | 2.55 | .0336 | .76 | .0059 | .054 |

2) Run 2, open jet (Fig. 13).

| Lift Gauge | L (lbs.) | Yaw Gauge | $M_y$ (in.lbs.) | Roll Gauge | $M_R$ (in.lbs.) | $h_{cm}$ | q | $C_L$ | $C_y$ | $C_R$ |
|---|---|---|---|---|---|---|---|---|---|---|
| 2.0 | .04 | 100 | 0 | - | - | 3.25 | .0406 | .03 | 0 | - |
| 10.5 | .25 | 99.0 | .032 | 71.5 | .83 | 3.27 | .0408 | .17 | .0018 | .047 |
| 18.5 | .44 | 98.2 | .055 | 71.5 | .83 | 3.27 | .0408 | .30 | .0031 | .047 |
| 29.5 | .69 | 97.2 | .088 | 71.0 | .835 | 3.30 | .0412 | .47 | .0050 | .047 |
| 38.5 | .91 | 96.2 | .110 | 70.0 | .86 | 3.30 | .0412 | .61 | .0062 | .0485 |
| 45.5 | 1.08 | 94.8 | .140 | 69.0 | .89 | 3.30 | .0412 | .73 | .0079 | .050 |
| 49.0 | 1.16 | 94.0 | .160 | 71.0 | .835 | 3.30 | .0412 | .78 | .0090 | .047 |

## DISCUSSION OF RESULTS AND COMPARISON WITH THEORY

The results of all runs made, of which two typical examples are shown in Figs. 12 and 13, are plotted in Figs. 14, 15, 16, and 17.

Since the tests with aileron angle a = 21° show considerable scatter and somewhat erratic variation between closed and open tunnel, only the runs with a = 14° will be used for comparison with the theory.

The yawing moment curves for a = 14° have been approximated by straight lines (Fig. 18), taking the average of all plotted points. The two rolling moment curves also represent average lines for a = 14°.

According to the theory of Stewart, the wall-effect correction for yawing moments is proportional to the product $C_R C_L$. Therefore the results shown in Fig. 18 have been replotted in Fig. 19 by plotting the difference $2 \Delta C_y$ against this product. The theoretical value of the slope of this curve is calculated below. Two different assumptions are made for the radius of the equivalent circular tunnel: 1) The half-width h/2 is taken as the radius, 2) the value $(2/\sqrt{\pi})$ (h/2), i.e., the radius of a circular tunnel of equal area, is taken as the radius. It is believed that the first assumption causes the interference effect to be overestimated slightly, while the second causes it to be underestimated. These conjectures can be verified when the theoretical calculations for square tunnels mentioned previously are completed.

The wall-effect correction for rolling moments is a constant for various $C_L$, according to Biot's theory (Reference 2). The correction $\Delta C_R/C_R$ as calculated by the theory, is also plotted against $C_L$ in Fig. 20 (dash - lines). For the radius of the tunnel the same two values were substituted as previously in the calculations of the yawing moment corrections:

1) Radius = h/2 corresponding to upper dash - line.

2) Radius = $\frac{2}{\pi}$ h/2 corresponding to lower dash - line.

The first assumption, radius = h/2, gives a value for the correction that is probably overestimated. The second assumption, radius = $(2/\pi)\times(h/2)$, probably underestimates the interference effect slightly.

These problems will be cleared after the aforementioned theoretical investigation on wall corrections for square wind tunnels is completed.

Tabulated Values for $2\Delta C_y$ and $\frac{\Delta C_R}{C_R}$ Curves.

| $C_L$ | $2\Delta C_y$ | $C_R$ $C_L$ mean | $2\Delta C_R$ | $C_R$ | $\frac{\Delta C_R}{C_R}$ |
|---|---|---|---|---|---|
| .2 | .0005 | .01 | .0050 | .0025 | .50 |
| .4 | .0011 | .02 | .0052 | .0026 | .52 |
| .6 | .0016 | .03 | .0040 | .0020 | .40 |
| .8 | .0021 | .04 | .0050 | .0025 | .50 |

Calculation of Theoretical Value of $\Delta C_y$ (See Reference 1).

1) Radius = h/2

Span b = 12 in.

$a_2$ = 2.5 in. (See Drawing of Wing Fig. 1a).

$a_1$ = 2.5 in.

Wing Area S = 36 in.$^2$

Half Width h/2 = 7 in.

$$\Delta C_{y1} = C_R C_L \frac{S\ (h/2)^2}{b^2\ (a_2^2 - a_1^2)} \left\{ F_1 \left( \frac{b a_2}{2\ (h/2)^2} \right) - F_1 \left( \frac{b a_1}{2\ (h/2)^2} \right) \right\}$$

$$= C_R C_L \frac{36 \times 49}{144\ (5.2^2 - 2.5^2)} \left\{ F_1 \frac{12 \times 5.5}{2 \times 49} - F_1 \frac{12 \times 2.5}{2 \times 49} \right\}$$

$$F_1 \frac{12 \times 5.5}{2 \times 49} = F_1\ (.673) = -.325$$ (Function F1() from Graph Reference 1).

$$F_1 \frac{12 \times 2.5}{2 \times 49} = F_1\ (.306) = -.422$$

$$= C_R C_L \times .51 \left\{ -.325 + .422 \right\}$$

$$\Delta C_{y1} = .0495\ C_R C_L$$

$$\Delta C_{y2} = \frac{S}{a_2^2 - a_1^2} \left\{ F_2 \left( \frac{b a_2}{2(h/2)^2} \right) - F_2 \left( \frac{b a_1}{2(h/2)^2} \right) \right\}$$

$$= C_R C_L \frac{36}{5.5^2 - 2.5^2} \left\{ F_2\ (.673) - F_2\ (.306) \right\}$$

$F_2$ (.673) = .092 (Function $F_2$ () from Graph Reference 1).

$F_2$ (.306) = .082

$$\Delta C_{y2} = C_R C_L \ 1.5 \left\{ .092 - .082 \right\}$$

$$= .015 \ C_R C_L$$

Total Correction:

$$\Delta C_y = \Delta C_{y1} + \Delta C_{y2} = \underline{\underline{.0645 \ C_R C_L}}.$$

2) Radius $= \dfrac{2 \times h}{\sqrt{\pi} \times 2} = 7.9$ in.

$$\Delta C_{y1} = C_R C_L \frac{36 \times 62.4}{144\,(5.5^2 - 2.5^2)} \left\{ F_1 \frac{12 \times 5.5}{2 \times 62.4} - F_1 \frac{12 \times 2.5}{2 \times 62.4} \right\}$$

$$= C_R C_L \times .65 \left\{ F_1(.53) - F_1(.24) \right\}$$

$$= C_R C_L \times .65 \left\{ - .385 + .425 \right\}$$

$$\Delta C_{y1} = .024\ C_R C_L$$

$$\Delta C_{y2} = C_R C_L \frac{36}{5.52 - 2.52} \left\{ F_2\,(.53) - F_2\,(.24) \right\}$$

$$= .0075\ C_R C_L$$

Total Correction:

$$\Delta C_y = \Delta C_{y1} + \Delta C_{y2} = \underline{\underline{.0315\ C_R C_L}}$$

Calculation of Theoretical Value of $\Delta C_R$. (See Reference 2).

1) Radius = h/2

Data:

| | | |
|---|---|---|
| Span | = | 12 in. |
| Root Chord $t_{Root}$ | = | 4 in. |
| Tip Chord $t_{tip}$ | = | 2 in. |
| Half Width of Tunnel h/2 | = | 7 in. |

$$\frac{\Delta C_R}{C_R} = \frac{b^3 t_{Root}}{2h^2(a_2^2 - a_1^2)} K_1\left(\frac{t_{Tip}}{t_{Root}}\right)\left\{K\left(\frac{a^2}{h/2}\right) - K\left(\frac{a_1}{h/2}\right)\right\}$$

$$= \frac{12^3 \times 4}{2 \times 14^2 (5.5^2 - 2.5^2)} K_1(.5)\left\{K\frac{5.5}{7} - K\frac{2.5}{7}\right\}$$

$K_1$ (.5) = .187 (Functions $K_1$ () and K () from Graph Reference 2).

K (.785) = .980

K (.357) = .120

$$\frac{\Delta C_R}{C_R} = \frac{1728 \times 4}{2 \times 196 \times 24} \times .187 \left\{.98 - .12\right\}$$

$$= \underline{\underline{.118}}$$

2) Radius $= \dfrac{2 \cdot h}{\sqrt{\pi} \cdot 2} = 7.9$ in.

$$\frac{\Delta C_R}{C_R} = \frac{12^3 \times 4}{2 \times 250 \,(5.5^2 - 2.5^2)} \; K_1(.5) \left\{ K\frac{5.5}{7.9} - K\frac{2.5}{7.7} \right\}$$

$K_1(.5) = 187$ (Functions $K_1()$ and $K()$ from Graph Reference 1).

$K(.696) = .63$

$K(.316) = .10$

$$\frac{\Delta C_R}{C_R} = .575 \times .187 \times .53 = \underline{\underline{.057}}$$

## CONCLUSION

The results of this work do not show definite quantitative agreement with the theory, although the qualitative variation of the interference effects with $C_L$ and $C_R$ has been verified. Both of the assumptions made above in calculating the theoretical results lead to values greater than the experimental ones. However, the values corresponding to the second assumption lie close to the experimental curves. The range included between the two assumptions is too large to allow any definite conclusion regarding the accuracy of the theories before the additional theoretical calculations now in progress have been completed. However, it can be concluded that application of the present theories to square wind tunnels should be made by taking as the effective radius a value of approximately $(2/\sqrt{\pi})(h/2)$.

It is probable that the scatter of the experimental points, especially those at 21° aileron deflection might be reduced by running the model at higher speeds, 100 to 120 m.p.h.; the accuracy of force and moment indication of the springs being greater for larger forces. In that case, however, a heavier damping would have to be installed in all balance components to avoid flutter of the model wing.

## REFERENCES

1. H.J. Stewart: "A Correction to the Yawing Moment Due to Ailerons for Circular Wind Tunnels." J. Ae. Sc. Number 8, June 1939, pages 329-331.

2. M. Biot: "Korrektur für das Quermoment von Tragflügeln bei Untersuchungen im Windkanal mit Kreisquerschnitt." Z F M, Nov. 15, 1933, pages 410-411.

3. J.S. Atsumi: "A Description of a Small Return Type Wind Tunnel at the California Institute of Technology." 1938 (To be published shortly.)

## INDEX OF FIGURES

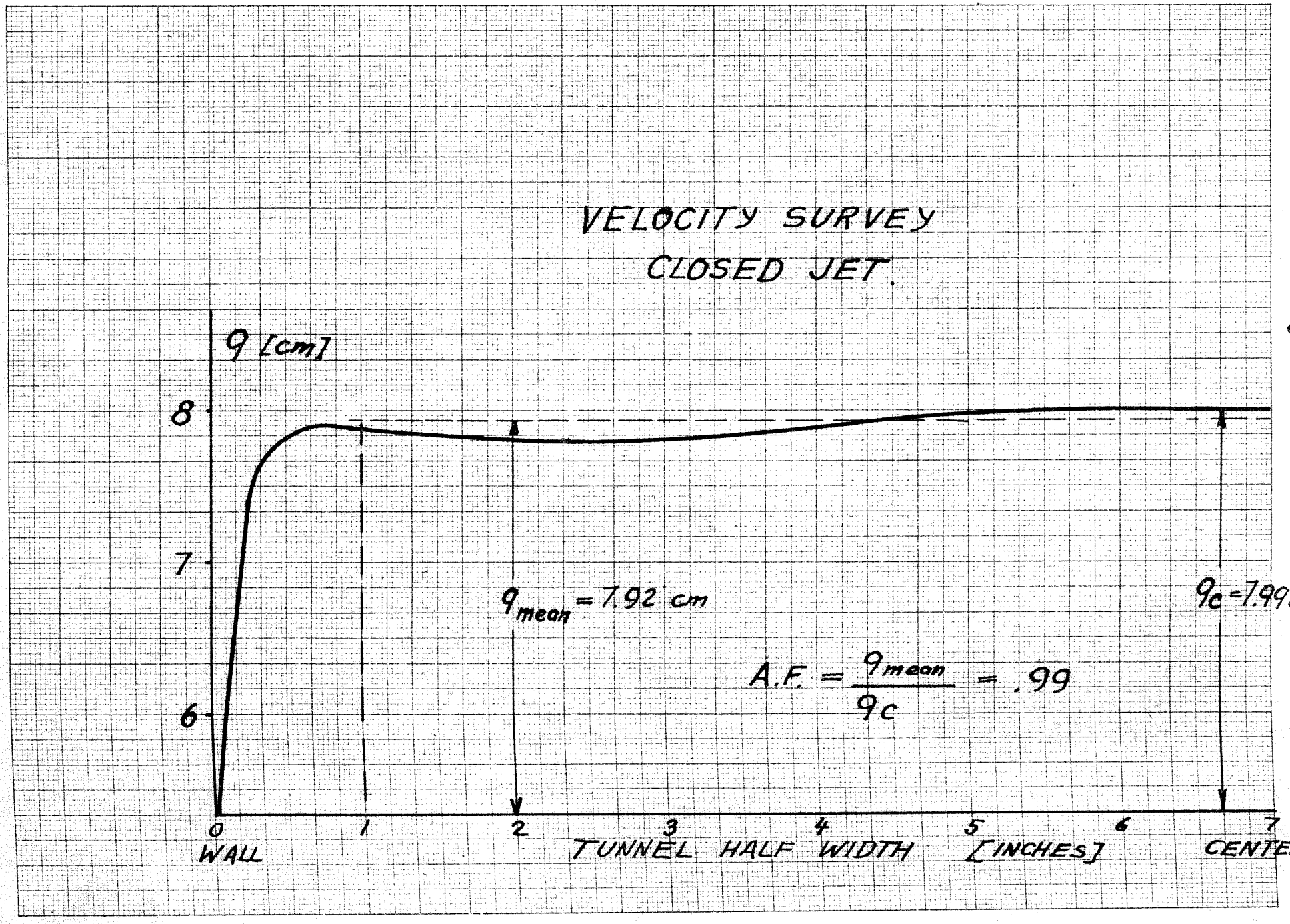
VELOCITY SURVEY
CLOSED JET.
q [cm]
8
7
6
$q_{mean} = 7.92$ cm
$q_c = 7.99$ cm
$A.F. = \frac{q_{mean}}{q_c} = .99$
0
WALL
1
2
3
4
5
6
7
CENTER
TUNNEL HALF WIDTH [INCHES]

Fig. 8

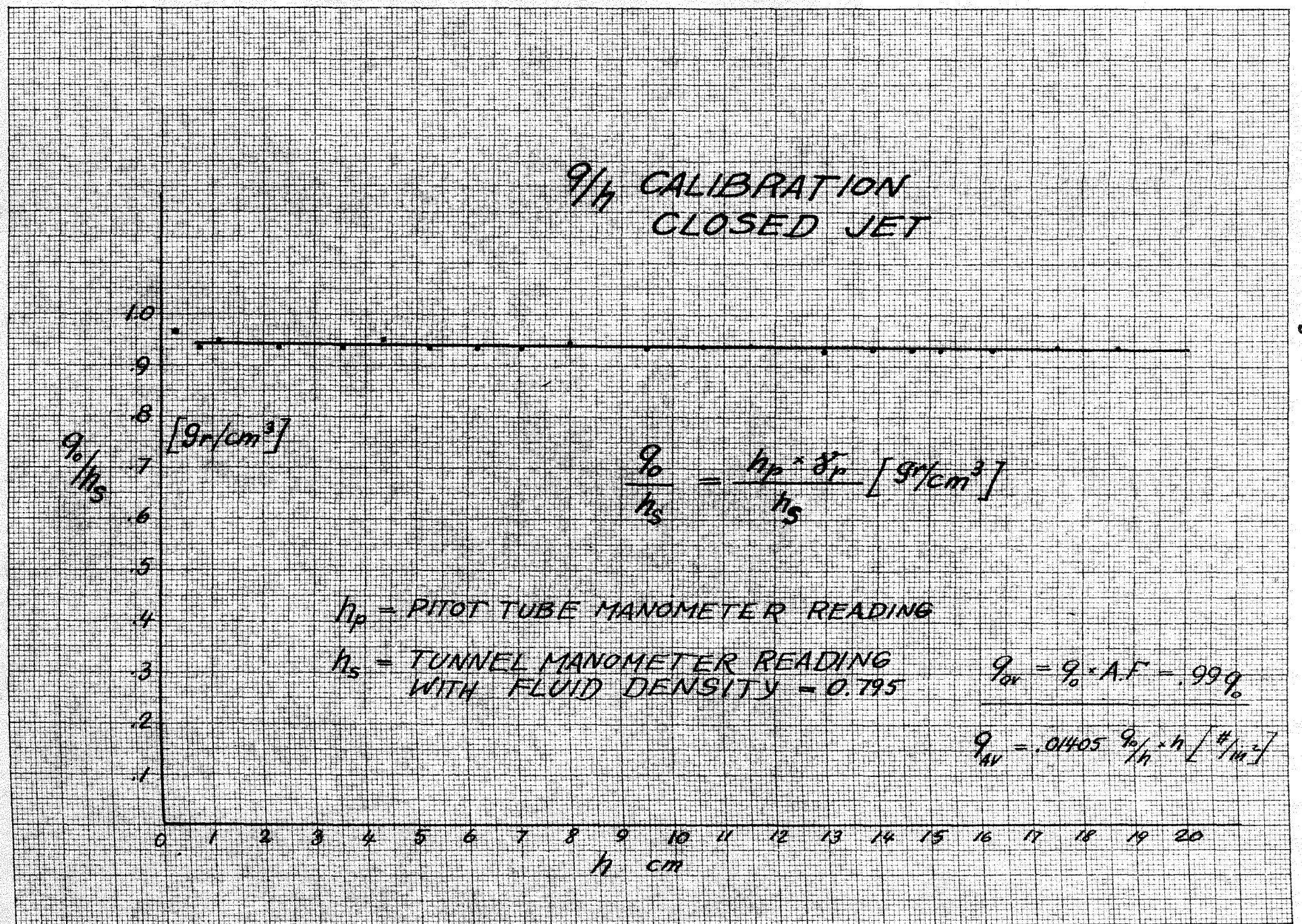
q/h CALIBRATION
CLOSED JET
1.0
.9
.8
.7
.6
.5
.4
.3
.2
.1
$q_o/h_s$ [gr/cm³]
0 1 2 3 4 5 6 7 8 9 10 11 12 13 14 15 16 17 18 19 20
h cm
$\frac{q_o}{h_s} = \frac{h_p \times \delta_r}{h_s}$ [gr/cm³]
$h_p$ = PITOT TUBE MANOMETER READING
$h_s$ = TUNNEL MANOMETER READING WITH FLUID DENSITY = 0.795
$q_{or} = q_o \times A.F = .99 q_o$
$q_{4v} = .01405\ q_{o/h} \times h$ [#/in²]

Fig. 9

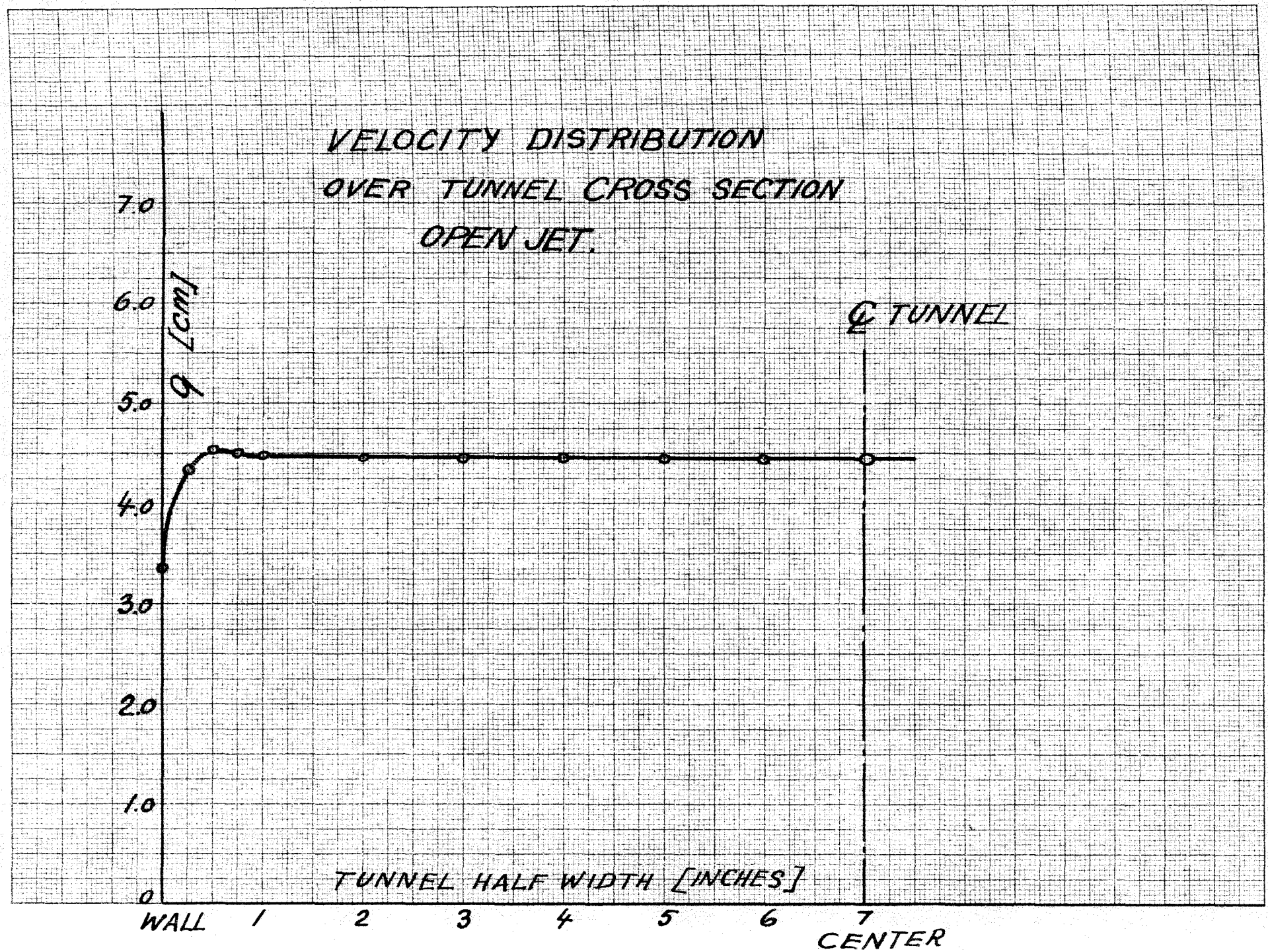
VELOCITY DISTRIBUTION
OVER TUNNEL CROSS SECTION
OPEN JET.
q [cm]
7.0
6.0
5.0
4.0
3.0
2.0
1.0
0
℄ TUNNEL
TUNNEL HALF WIDTH [INCHES]
WALL
1
2
3
4
5
6
7
CENTER

Fig. 10

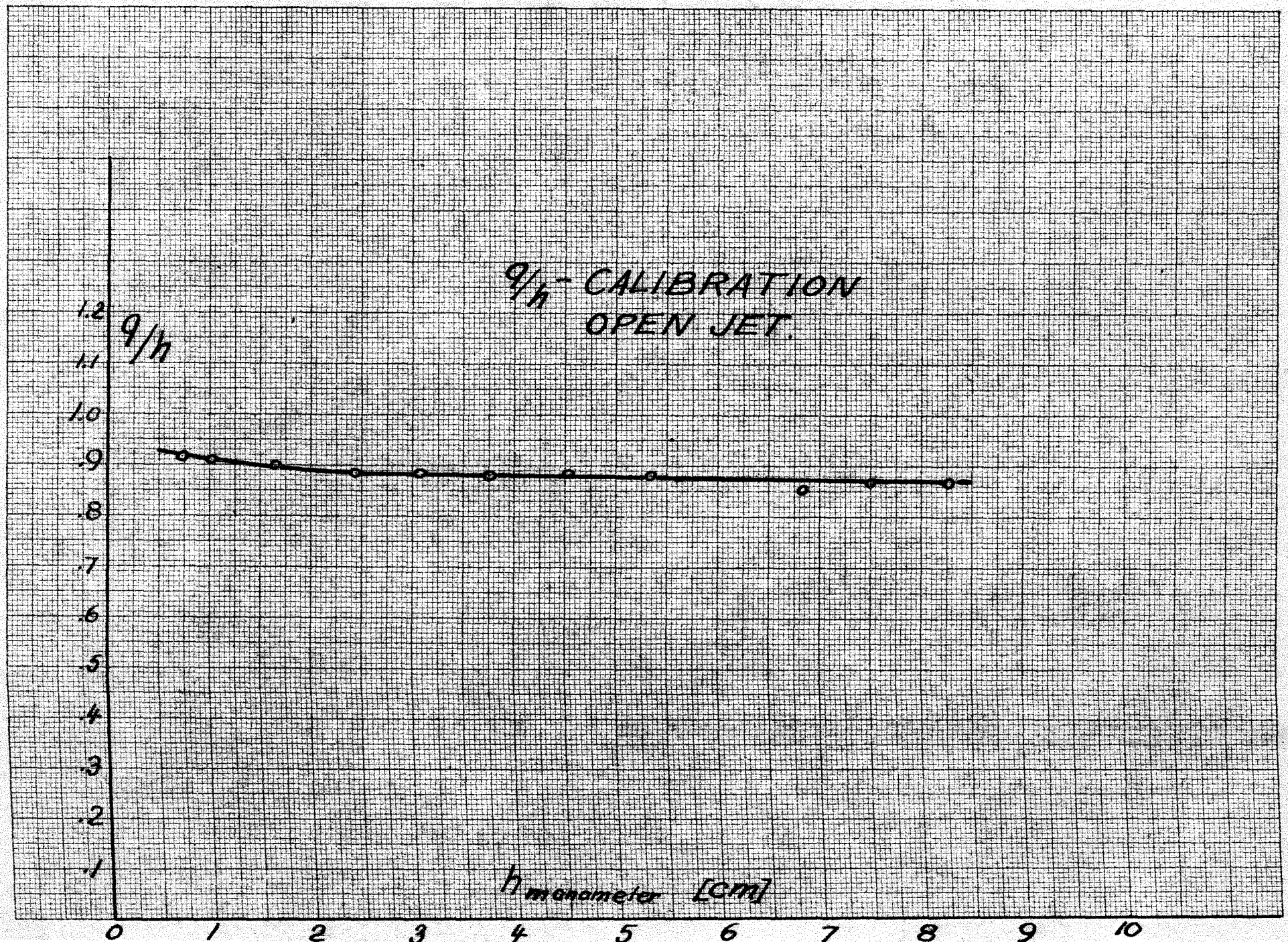
q/h - CALIBRATION
OPEN JET.
q/h
1.2
1.1
1.0
.9
.8
.7
.6
.5
.4
.3
.2
.1
h manometer [cm]
0
1
2
3
4
5
6
7
8
9
10

Fig. 11

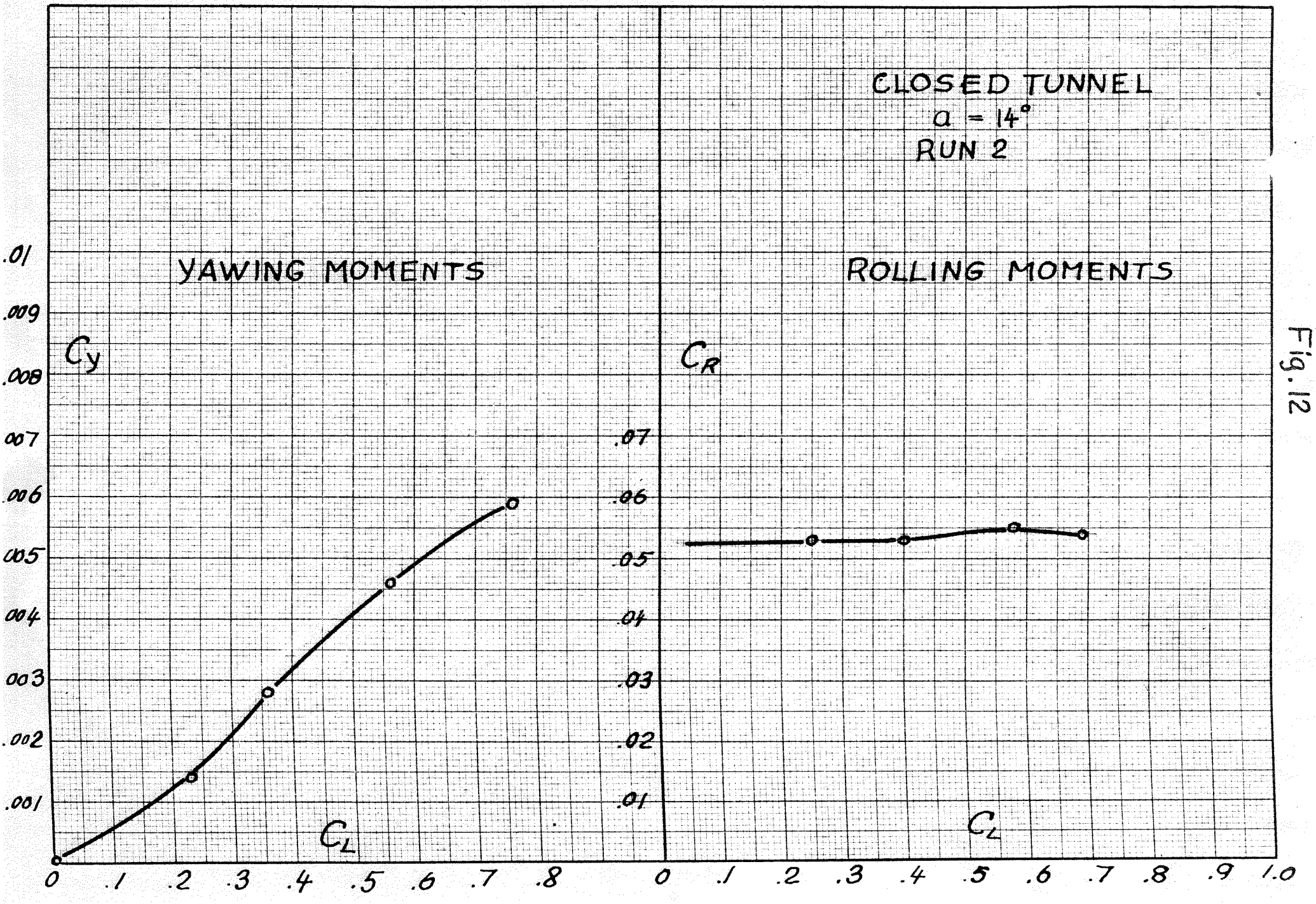
CLOSED TUNNEL
α = 14°
RUN 2
YAWING MOMENTS
ROLLING MOMENTS
$C_y$
$C_R$
$C_L$
$C_L$
.01
.009
.008
007
006
005
004
003
.002
.001
.07
.06
.05
.04
.03
.02
.01
0 .1 .2 .3 .4 .5 .6 .7 .8
0 .1 .2 .3 .4 .5 .6 .7 .8 .9 1.0

Fig. 12

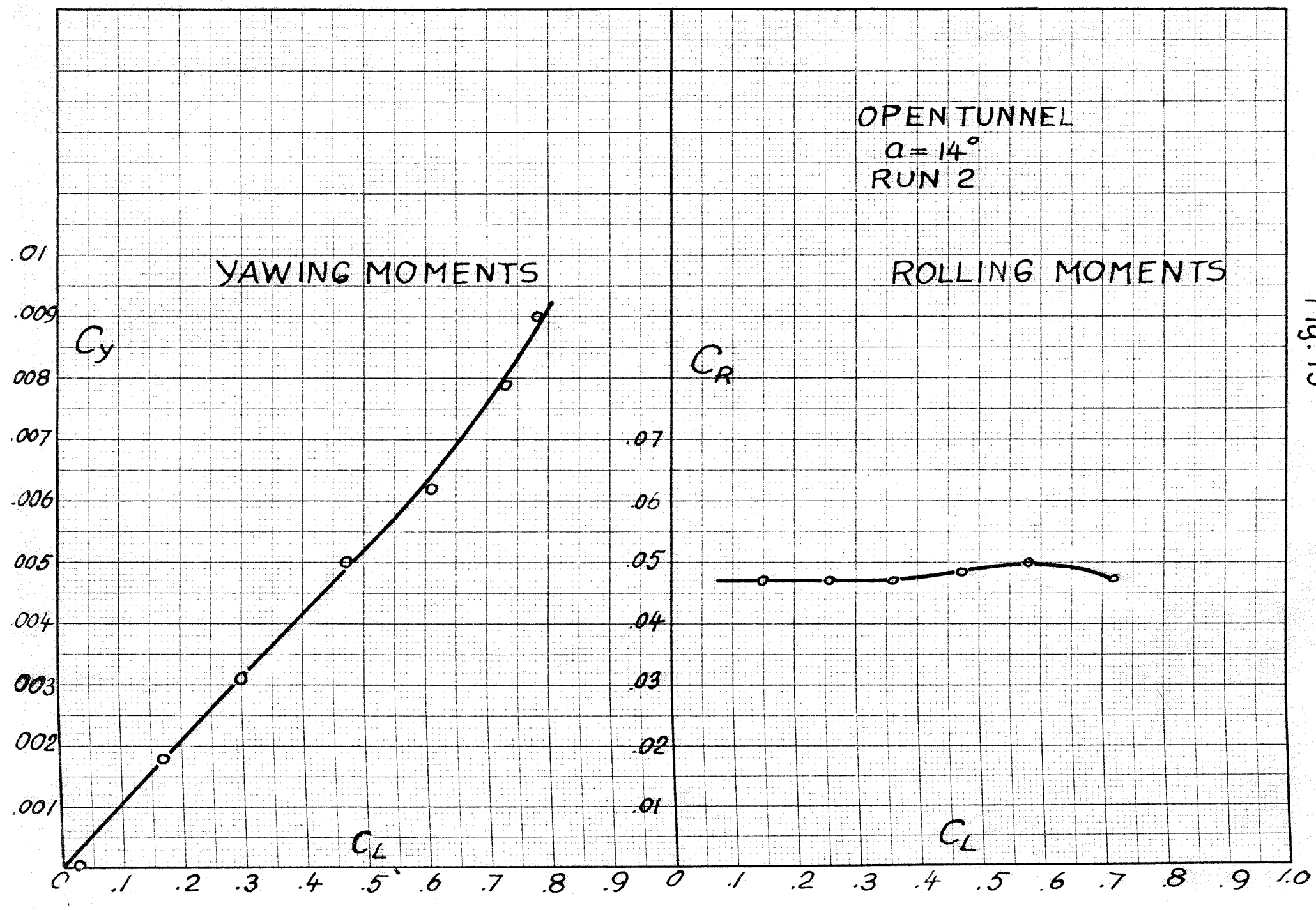
OPEN TUNNEL
α = 14°
RUN 2
YAWING MOMENTS
ROLLING MOMENTS
$C_y$
$C_R$
$C_L$
$C_L$
.01
.009
.008
.007
.006
.005
.004
.003
.002
.001
.07
.06
.05
.04
.03
.02
.01
0 .1 .2 .3 .4 .5 .6 .7 .8 .9
0 .1 .2 .3 .4 .5 .6 .7 .8 .9 1.0

Fig. 13

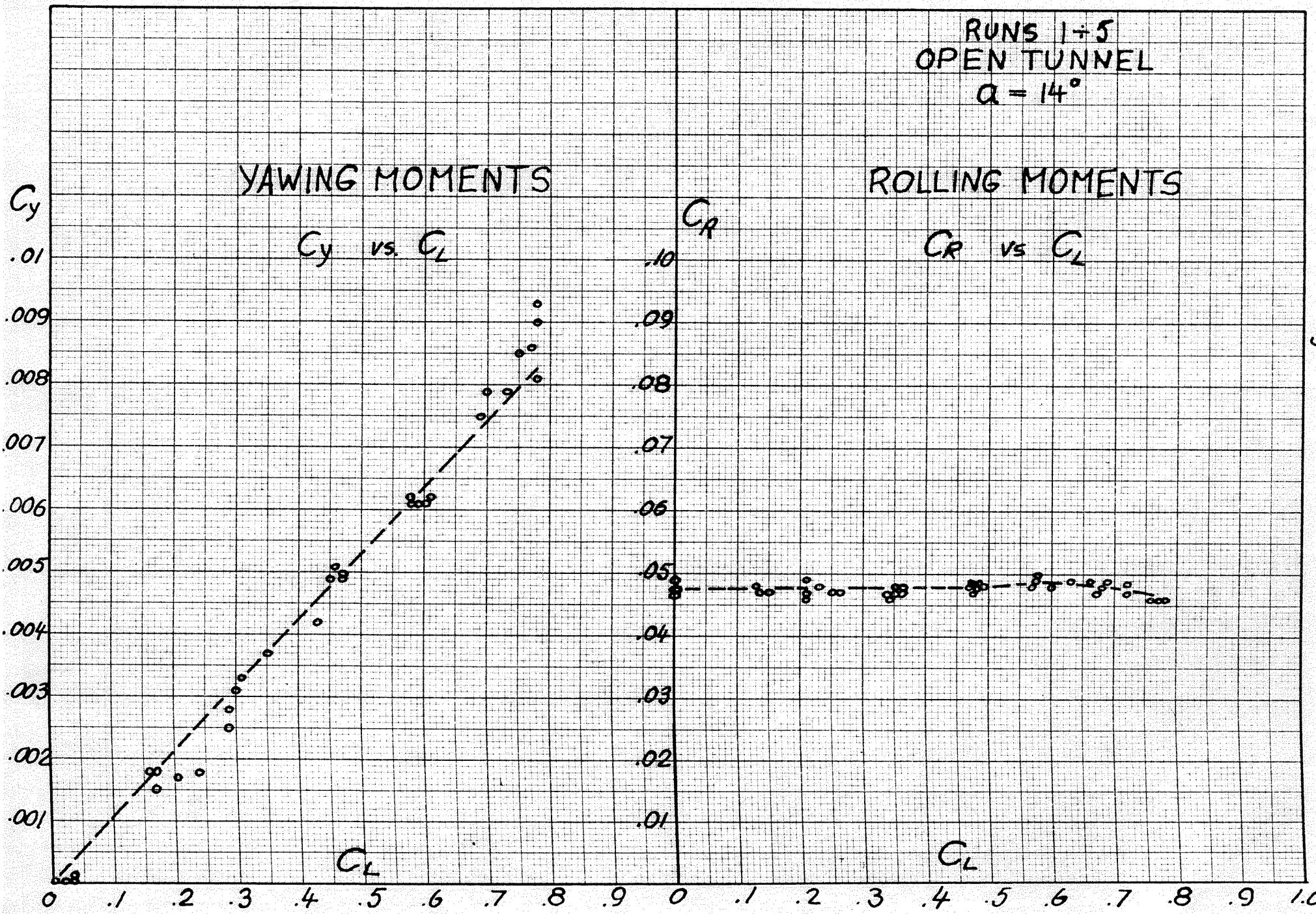
RUNS 1+5
OPEN TUNNEL
α = 14°
YAWING MOMENTS
$C_y$ vs. $C_L$
ROLLING MOMENTS
$C_R$ vs $C_L$
$C_y$
$C_R$
$C_L$
$C_L$
.01
.009
.008
.007
.006
.005
.004
.003
.002
.001
.10
.09
.08
.07
.06
.05
.04
.03
.02
.01
0 .1 .2 .3 .4 .5 .6 .7 .8 .9 0 .1 .2 .3 .4 .5 .6 .7 .8 .9 1.0

Fig. 14

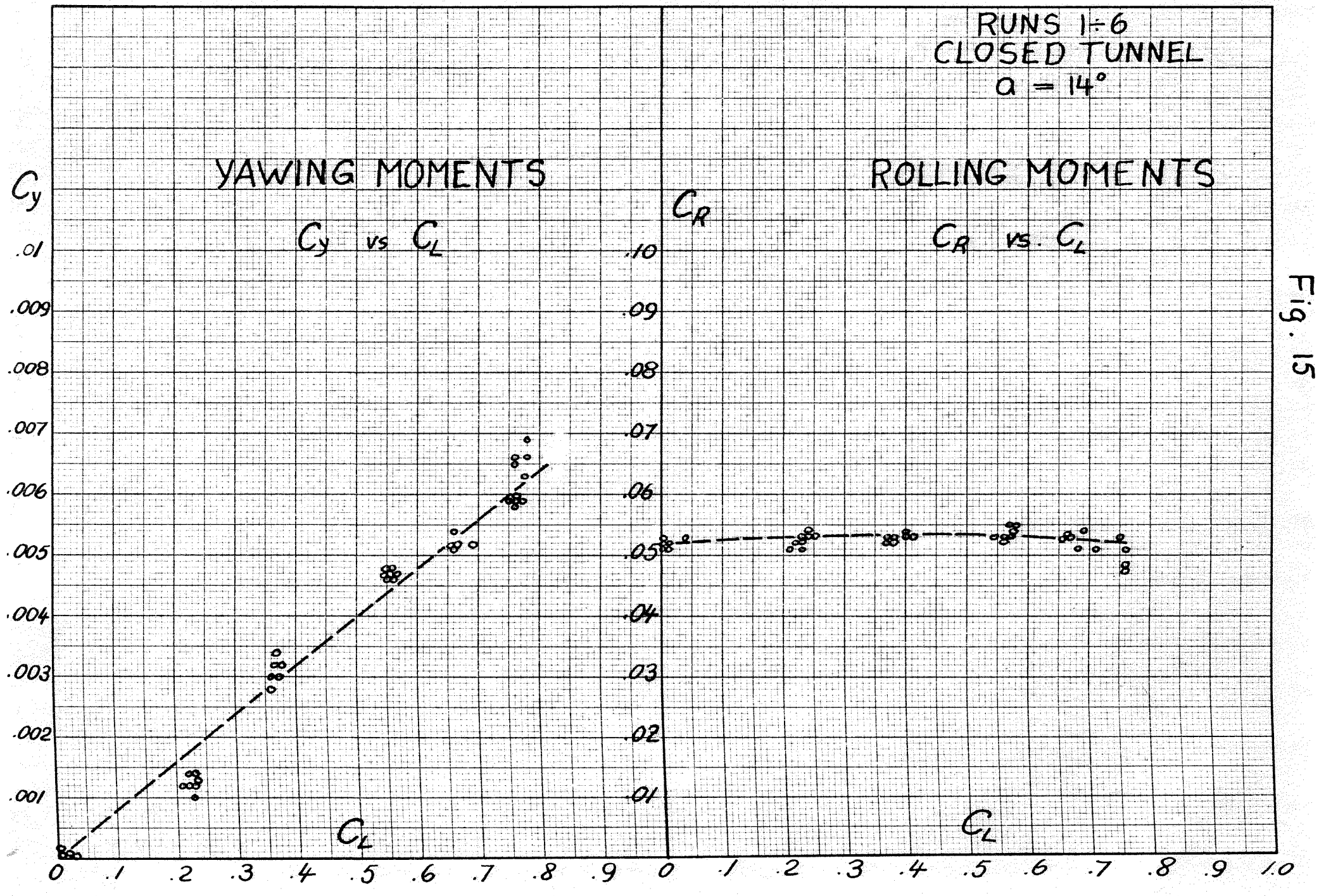
RUNS 1-6
CLOSED TUNNEL
α = 14°
YAWING MOMENTS
$C_y$ vs $C_L$
$C_y$
.01
.009
.008
.007
.006
.005
.004
.003
.002
.001
$C_L$
0 .1 .2 .3 .4 .5 .6 .7 .8 .9
ROLLING MOMENTS
$C_R$ vs. $C_L$
$C_R$
.10
.09
.08
.07
.06
.05
.04
.03
.02
.01
$C_L$
0 .1 .2 .3 .4 .5 .6 .7 .8 .9 1.0

Fig. 15

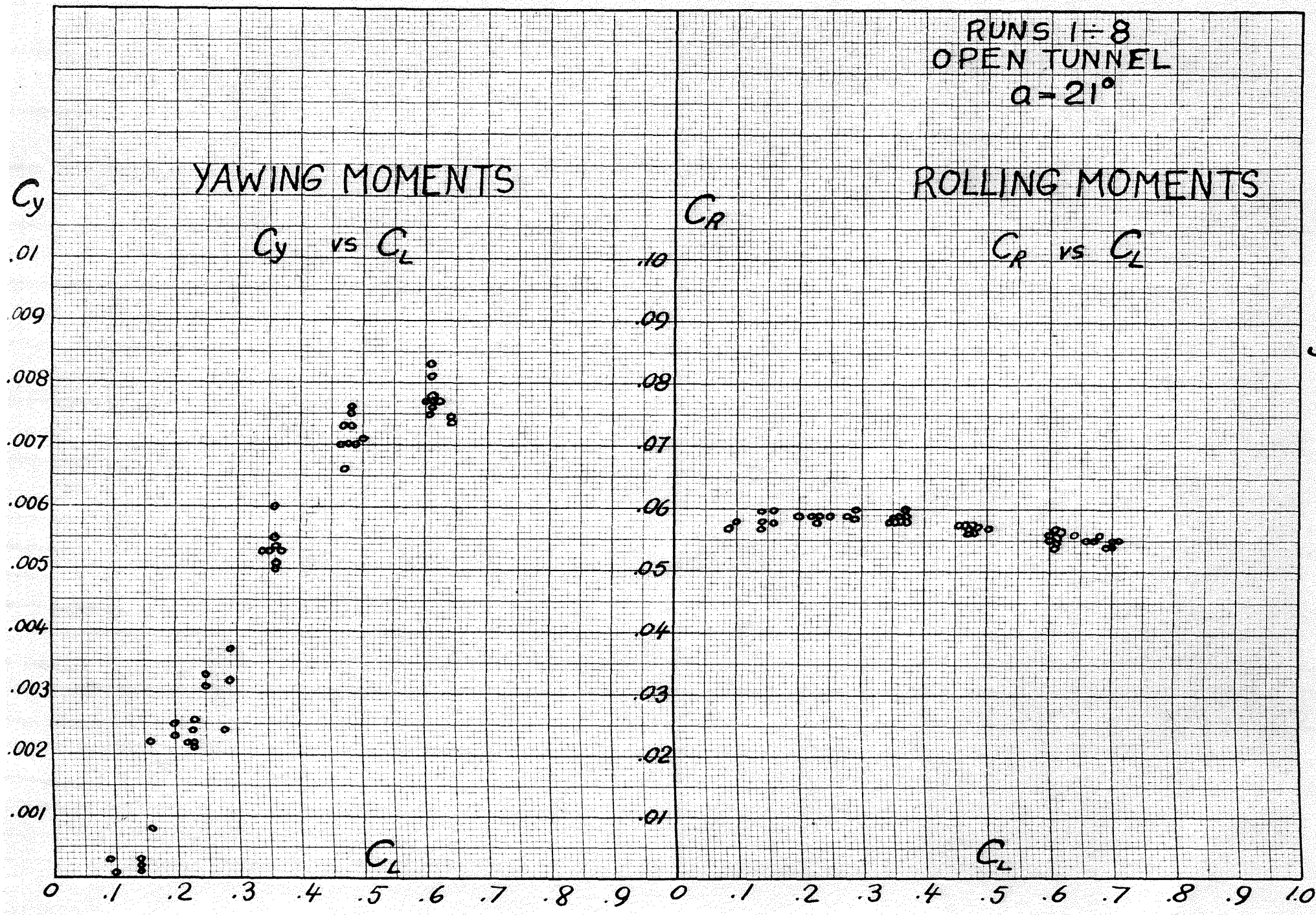
RUNS 1÷8
OPEN TUNNEL
α = 21°
YAWING MOMENTS
$C_y$ vs $C_L$
$C_y$
.01
.009
.008
.007
.006
.005
.004
.003
.002
.001
$C_L$
0 .1 .2 .3 .4 .5 .6 .7 .8 .9
ROLLING MOMENTS
$C_R$ vs $C_L$
$C_R$
.10
.09
.08
.07
.06
.05
.04
.03
.02
.01
$C_L$
0 .1 .2 .3 .4 .5 .6 .7 .8 .9 1.0

Fig. 16

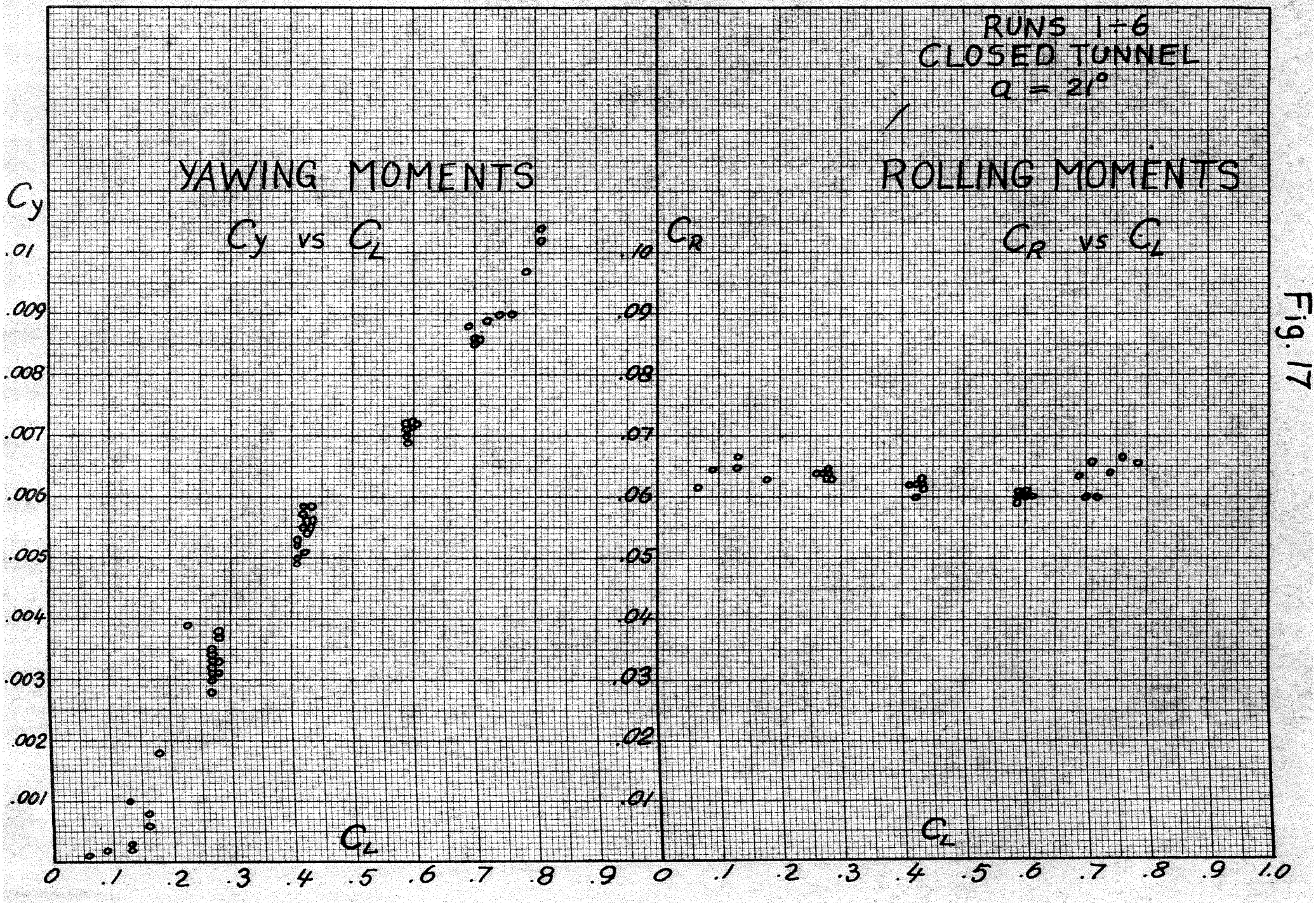
RUNS 1÷6
CLOSED TUNNEL
α = 21°
YAWING MOMENTS
$C_y$ vs $C_L$
$C_y$
.01
.009
.008
.007
.006
.005
.004
.003
.002
.001
$C_L$
0 .1 .2 .3 .4 .5 .6 .7 .8 .9
ROLLING MOMENTS
$C_R$ vs $C_L$
$C_R$
.10
.09
.08
.07
.06
.05
.04
.03
.02
.01
$C_L$
0 .1 .2 .3 .4 .5 .6 .7 .8 .9 1.0

Fig. 17

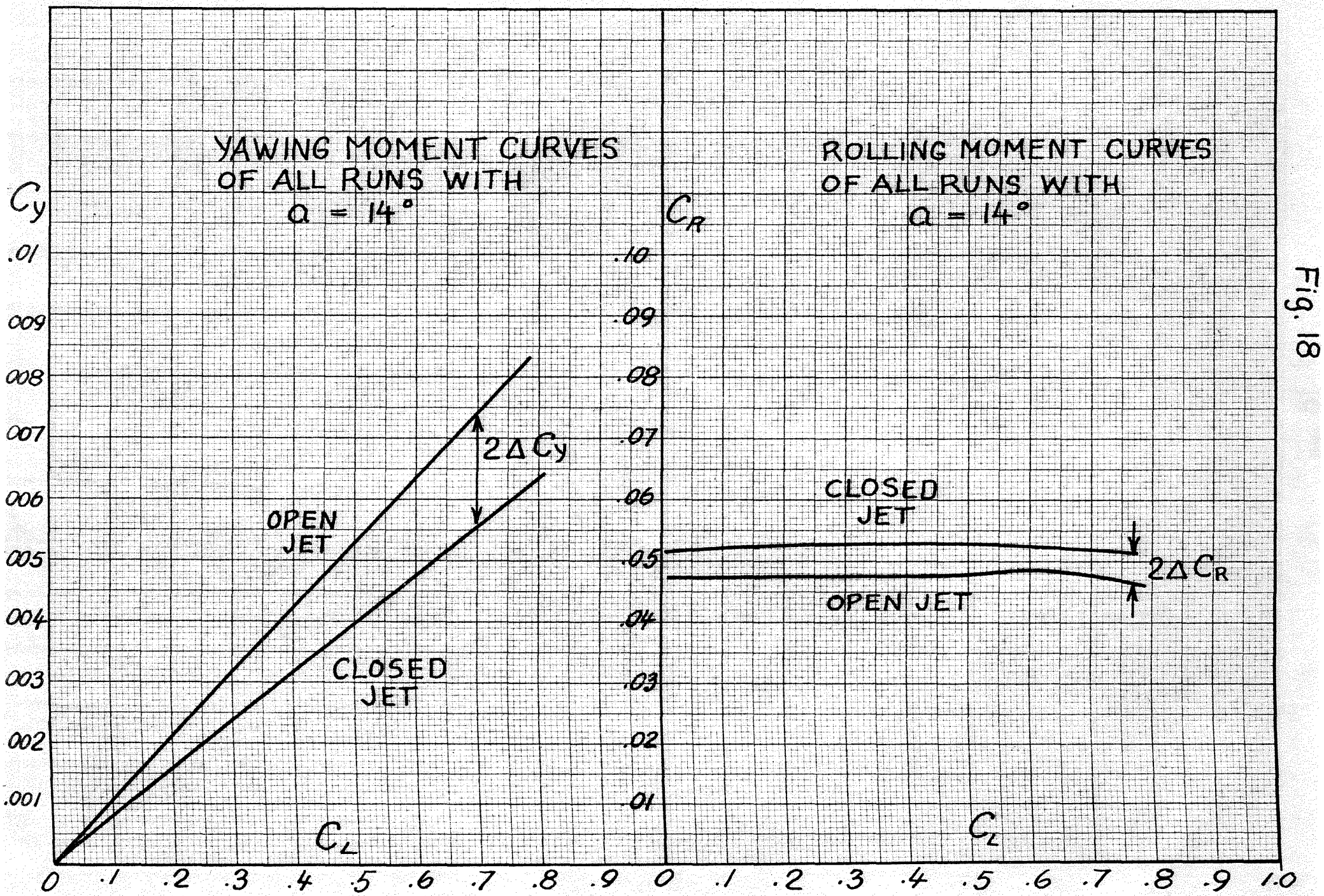
YAWING MOMENT CURVES
OF ALL RUNS WITH
α = 14°
$C_y$
.01
009
008
007
006
005
004
003
002
.001
$2\Delta C_y$
OPEN JET
CLOSED JET
$C_L$
0 .1 .2 .3 .4 .5 .6 .7 .8 .9
ROLLING MOMENT CURVES
OF ALL RUNS WITH
α = 14°
$C_R$
.10
.09
.08
.07
.06
.05
.04
.03
.02
.01
CLOSED JET
$2\Delta C_R$
OPEN JET
$C_L$
0 .1 .2 .3 .4 .5 .6 .7 .8 .9 1.0

Fig. 18

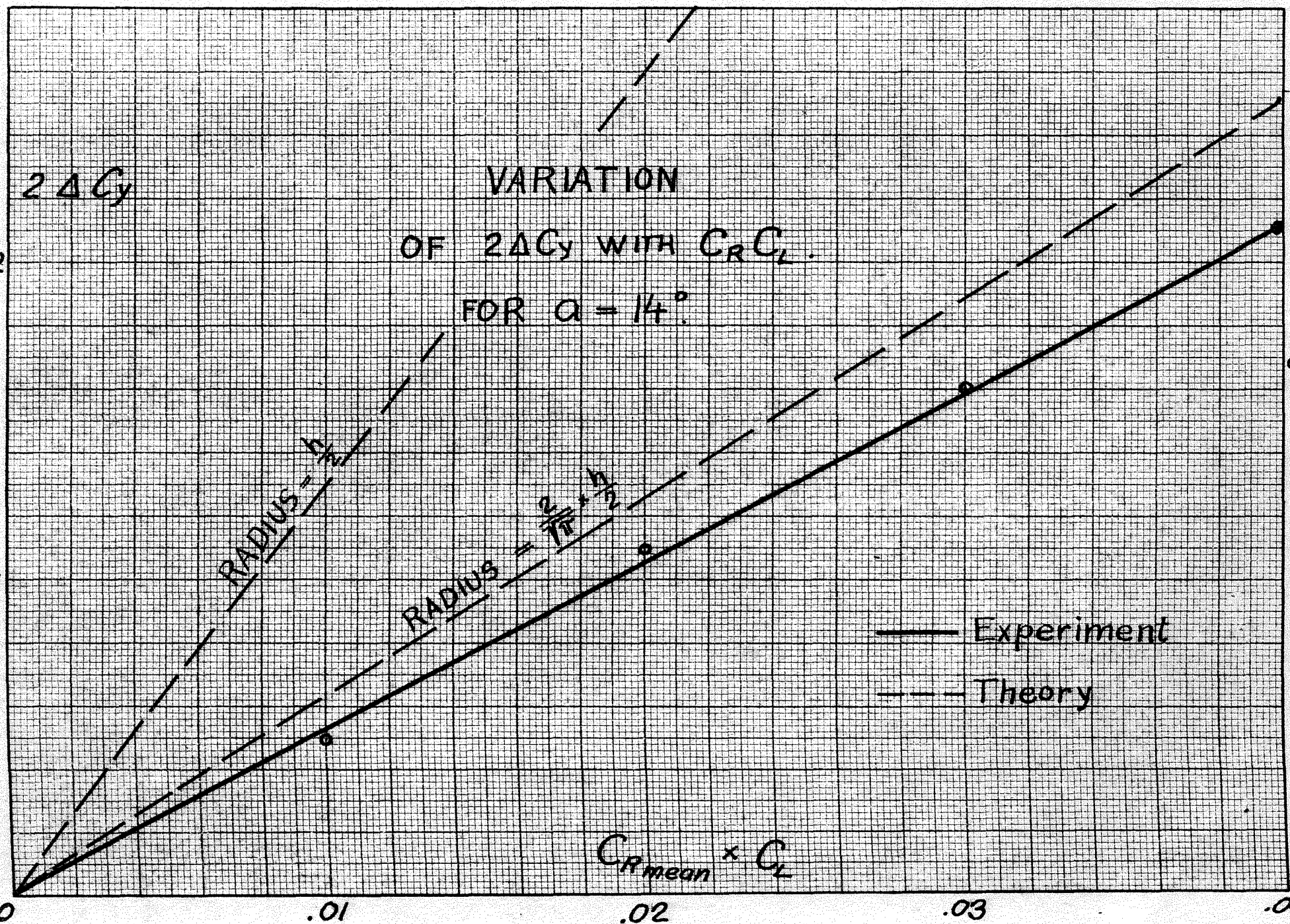
VARIATION
OF $2\Delta C_y$ WITH $C_R C_L$.
FOR $\alpha = 14°$.
$2\Delta C_y$
.002
.001
0
.01
.02
.03
.04
$C_{R\,mean} \times C_L$
RADIUS = $\frac{2}{\pi} h_w$
RADIUS = $\frac{2}{\pi} h_w + \frac{h}{2}$
Experiment
Theory

Fig. 19.

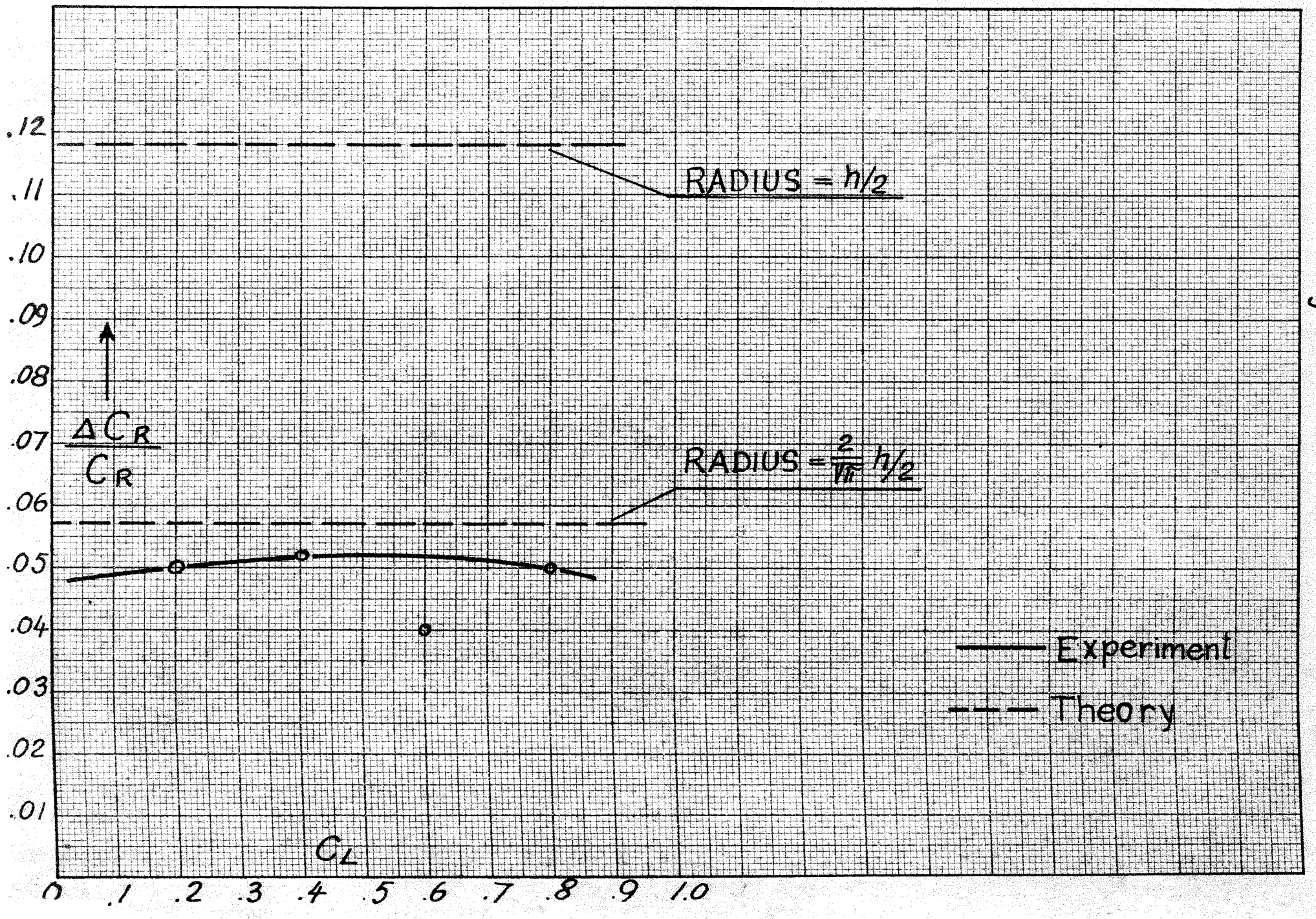
.12
.11
.10
.09
.08
.07
.06
.05
.04
.03
.02
.01
$\frac{\Delta C_R}{C_R}$
RADIUS = h/2
RADIUS = $\frac{2}{\pi}$ h/2
Experiment
Theory
$C_L$
0
.1
.2
.3
.4
.5
.6
.7
.8
.9
1.0

Fig. 20

Fig. 21

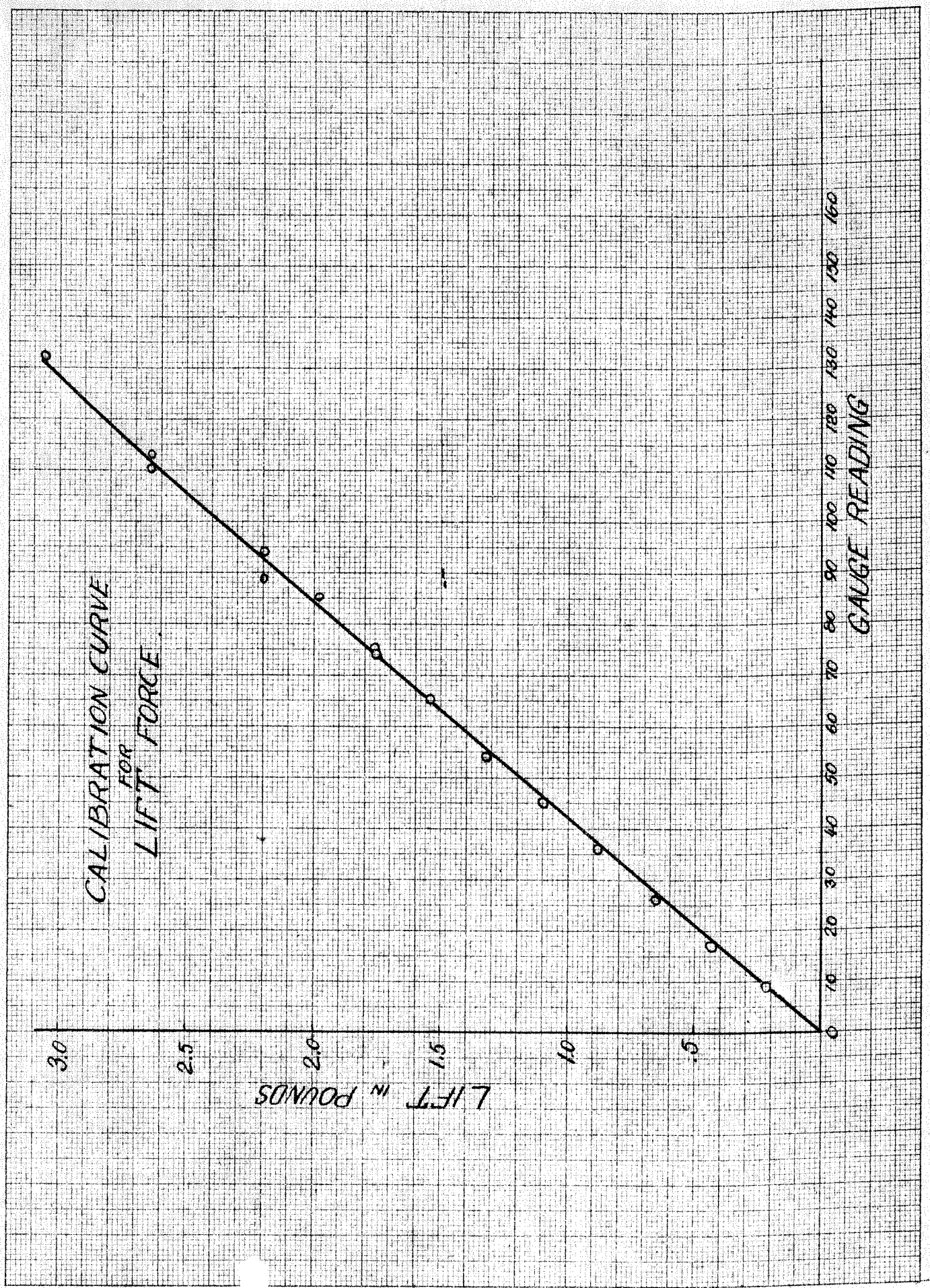
CALIBRATION CURVE
FOR
LIFT FORCE.
LIFT IN POUNDS
3.0
2.5
2.0
1.5
1.0
.5
0
10
20
30
40
50
60
70
80
90
100
110
120
130
140
150
160
GAUGE READING

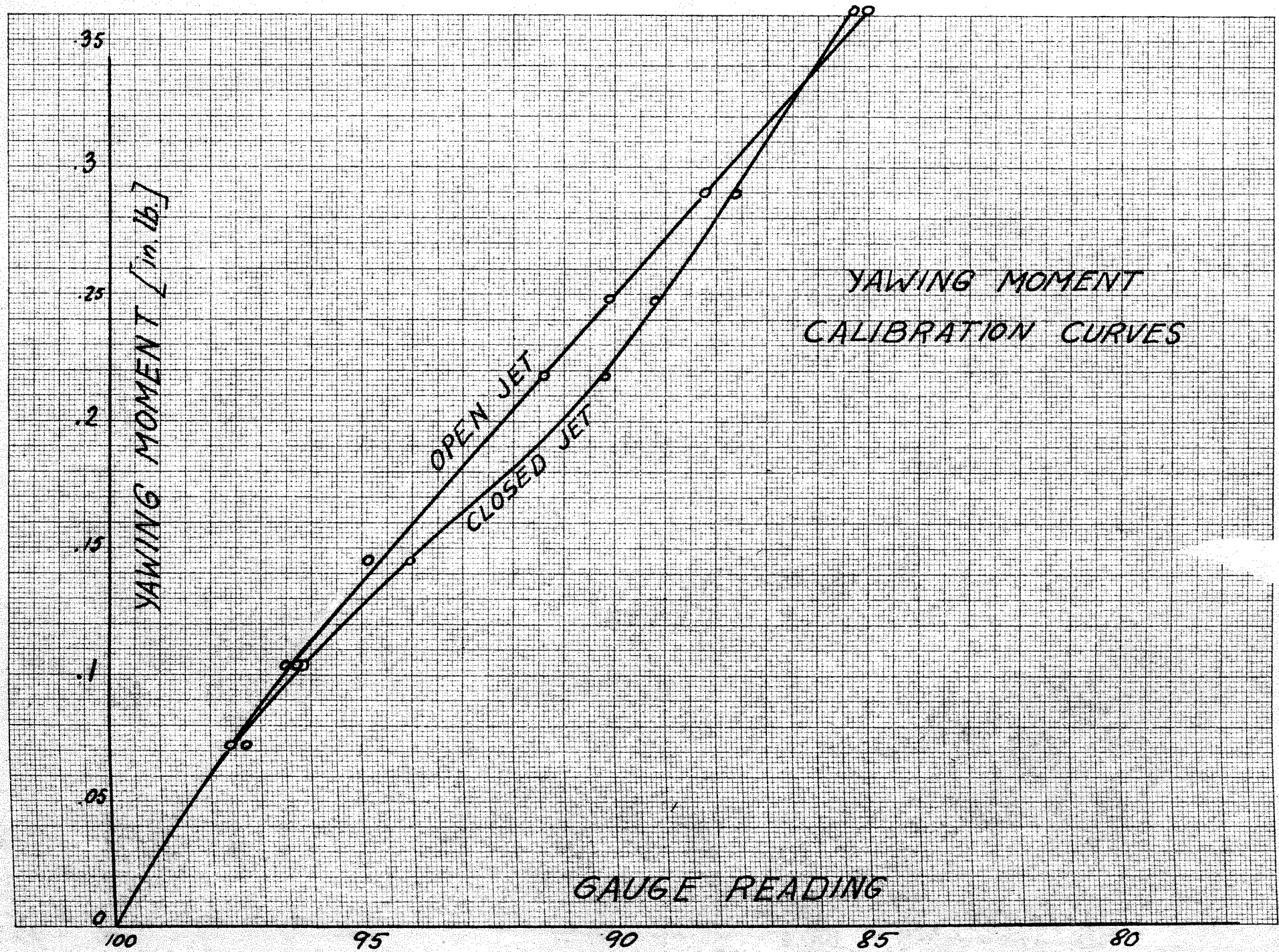
YAWING MOMENT CALIBRATION CURVES
YAWING MOMENT [in. lb.]
.35
.3
.25
.2
.15
.1
.05
0
OPEN JET
CLOSED JET
GAUGE READING
100
95
90
85
80

Fig. 22

Fig. 23.

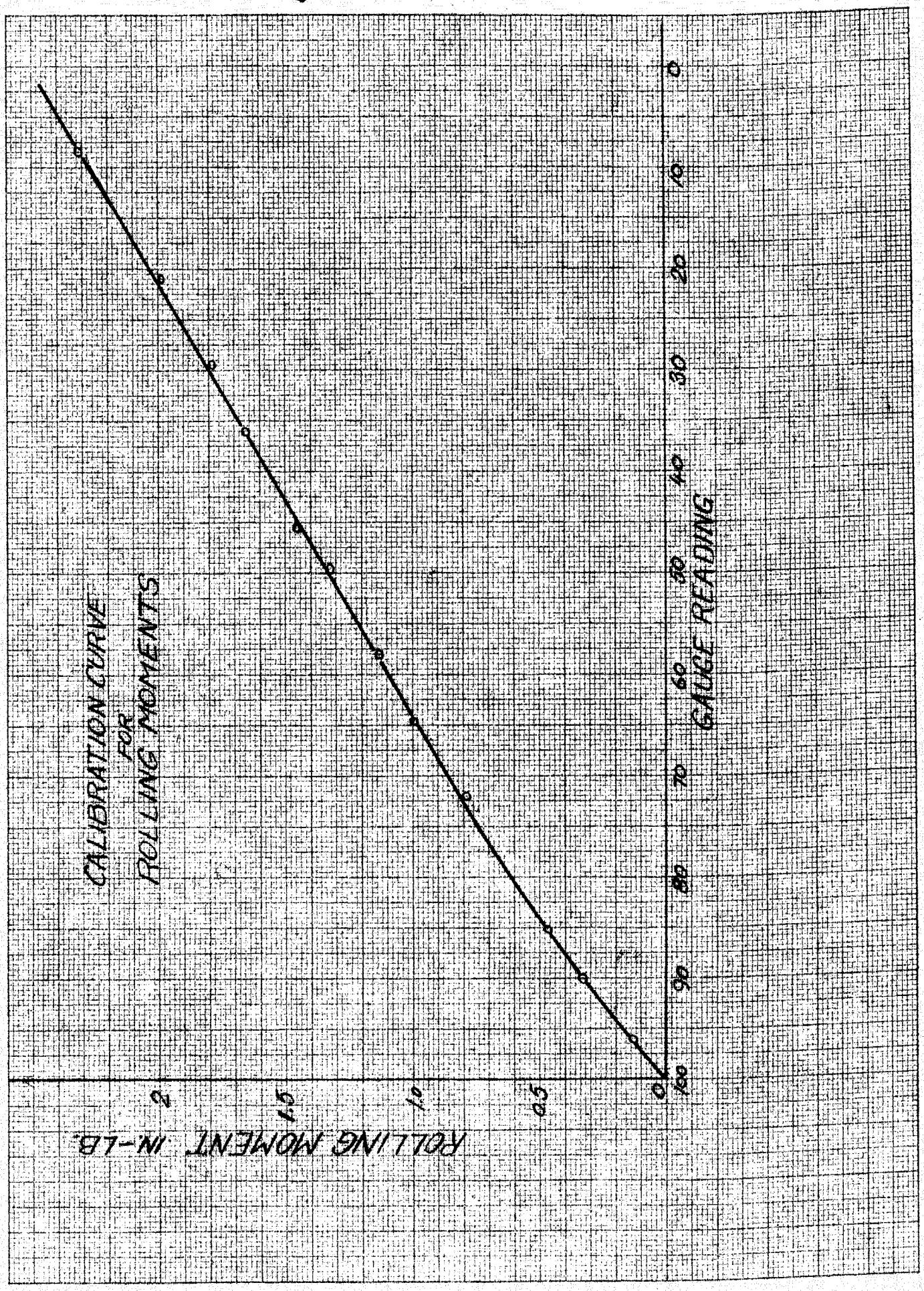
CALIBRATION CURVE
FOR
ROLLING MOMENTS
ROLLING MOMENT IN-LB.
2
1.5
1.0
0.5
0
GAUGE READING
0
10
20
30
40
50
60
70
80
90
100